

Active jamming of microswimmers at a bottleneck constrictionEdouardo Al Alam ¹, Marvin Brun-Cosme-Bruny ¹, Vincent Borne,¹ Sylvain Faure ²,
Bertrand Maury,^{3,2} Philippe Peyla ¹ and Salima Rafai ^{1,*}¹Université Grenoble Alpes, CNRS, LIPhy, F-38000 Grenoble, France²Laboratoire de Mathématiques d'Orsay, Université Paris-Saclay, 91405 Orsay Cedex, France³Département de Mathématiques Appliquées, Ecole Normale Supérieure, Université PSL, Paris, France

(Received 10 May 2022; accepted 14 September 2022; published 26 September 2022)

When attracted by a stimulus (light), microswimmers can build up very densely at a constriction and thus cause jamming. The microalga *Chlamydomonas Reinhardtii* is used here as a model system to study this phenomenon. Its negative phototaxis makes the algae swim away from a light source and go through a microfabricated bottleneck-shaped constriction. Successive jamming events interspersed with bursts of algae are observed. A power-law decrease describes well the distribution of time lapses of blockages. Moreover, the evacuation time is found to increase when increasing the swimming velocity. These results are reminiscent of crowd dynamics and, in particular, what has been called the faster is slower effect in the dedicated literature. It also raises the question of the presence of tangential solid friction between motile cells densely packed. Furthermore, we demonstrate the existence of a transition from a jammed phase described by a power-law decrease to an uninterrupted phase described by an exponential decay, we characterize such a transition as a function of door size and swimming velocity. Interestingly, the exponential flowing regime shows what might be referred to as “a faster is faster” regime.

DOI: [10.1103/PhysRevFluids.7.L092301](https://doi.org/10.1103/PhysRevFluids.7.L092301)

In biotechnologies, harvesting micro-organisms, such as bacteria [1] or microalgae [2] is now a tremendous challenge to extract new drugs and chemicals [3,4]. Several microfluidic devices have recently emerged to achieve such a task [5–7]. A jamming phase can often occur when concentrated cells are transported by a fluid [8–10]. At the microscale, jamming results from the accumulation of cells at a constriction, leading to the buildup of fouling layers. Jamming can severely disrupt the performance of microfluidic devices [11]. Initially, it reduces the permeability of channels or pores and eventually leads to a complete obstruction of the flow [12,13]. Jamming is, thus, one of the leading causes of efficiency loss in high-throughput technologies processes [14]. To remedy fouling and jamming, it is usually necessary to completely stop the process and use cleaning strategies that consume energy and time before restarting the process [15]. Motile cells (bacteria or microalgae) can self-accumulate without an external flow and can go to nest in a particular place of the circuit (pores, porous regions, constrictions), thus, forming an active jamming that is essential to characterize. Beyond jamming, this type of accumulation can be a precursor to formation of biofilms. More generally, jamming problems occur in extremely varied situations that are nowadays very much studied in the context of crowd dynamics. Crowd motion modeling has become a very active field of research, and serious debates on how to model certain behaviors, such as panic movements are still ongoing in the community [16]. In this particular case, the faster is slower (FiS) effect plays a central role: It essentially indicates that, in certain situations where the crowd is very dense, the

*salima.rafai@univ-grenoble-alpes.fr



FIG. 1. (a) Schematic of bottleneck-shaped microchannel of thickness $20\text{-}\mu\text{m} \sim 2 \times$ diameter of CR. The dashed rectangle represents the zone over which time lapses are measured. A light source is placed on the left, triggering a left to right swimming motion. (b) Snapshots of the jamming process through a $D = 10\text{-}\mu\text{m}$ constriction at different times.

willingness of individuals is to increase their speed when making an effort to evacuate, which has the effect of blocking the entire evacuation process. In addition, it has been established that these paradoxical effects observed in crowd dynamics persist in a very wide variety of systems: In a granular silo [17], in a suspension [18] as well as in a flock of sheep or in a crowd of pedestrians [19]. A physicist's approach is to look for a common physical mechanism behind these observable measured values. At a minimum, it would be desirable to succeed in defining universality classes in this family of problems. In particular, a class of systems could be that of active suspensions. In this Letter, we introduce active suspensions as a class of crowds and focus our study on jamming events occurring at a constriction due to cell buildup of microalgae. Understanding behavior of highly concentrated motile micro-organisms and especially their short-range interactions through adhesion or friction remains a challenge. In our experiments, we use a negative phototactic strain of green algae *Chlamydomonas reinhardtii* (CR) swimming away from light and moving toward a constriction [Fig. 1(b)]. We identify jamming events and analyze the dynamics of evacuation. The greater the velocity of the algae, the greater the active jamming. This phenomenon is very similar to the FiS effect mentioned above.

Experimental details. CR is a biflagellate photosynthetic cell [20] with diameter $a = 10 \mu\text{m}$. Cells are grown under a 14-h/10-h light/dark cycle at 22°C in *tris*acetate phosphate medium and are harvested in the middle of the exponential growth phase. CR's front flagella beat in a breaststroke manner and propel the cell in the fluid. The swimming is characterized by a persistent random walk in absence of bias [21,22]. However, in the presence of a light stimulus (green wavelength, i.e., around 510 nm), the strain used in this Letter (CC-124) tends to swim away from the light source and perform a ballistic motion [23], this is known as negative phototaxis. CR suspension is concentrated by centrifuging 40 mL at 1000 rpm for 15 min and removing the supernatant, the solution is then placed under a red light for 2 h. Velocity is controlled by increasing the medium's viscosity via Dextran addition [24,25]. Cells are finally introduced within a microfluidic device composed of two reservoir chambers of height $20 \mu\text{m}$ (twice the cell diameter) linked by a bottleneck constriction of varying width $D = 10, 20, 30,$ and $50 \mu\text{m}$ [Fig. 1(a)]. Microfabrication is made of transparent polydimethylsiloxane by means of soft lithography processes [26], Bovine serum albumin is used to passivate the device and avoid cells' adhesion.

We observe the cells under a bright field inverted microscope (Olympus IX71, magnification $\times 4$) coupled to a 14-bit CCD camera (Prosilica GX) used at a frame rate of 20 fps. The sample is enclosed in a black box with two red filtered windows for visualization in order to prevent the microscope light from triggering phototaxis.

The algae are initially distributed homogeneously in the chamber. A white LED light is switched on the left side of the sample. Negative phototaxis makes the microswimmers swim toward walls and at the constriction. Particle tracking is performed using the library TRACKPY [27,28]. The volume fraction of cells when very dense regimes are reached is deduced from gray level intensity measurements that were calibrated beforehand. Figure 1(b) illustrates one typical geometry of the experiments. The sequence shows a series of microscopy images at different timescales following the light stimulus. The microswimmers swim away from the light and toward the constriction (from

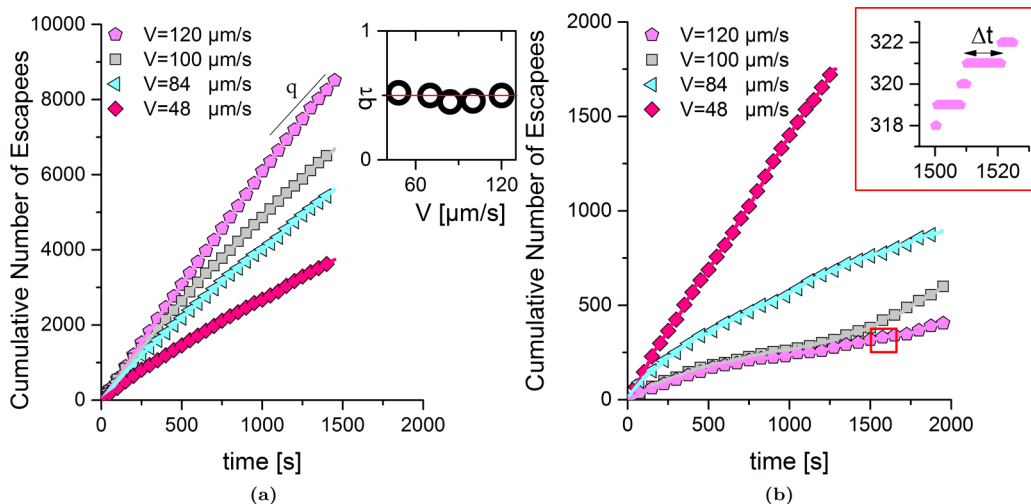


FIG. 2. Cumulative number of CR crossing the constriction as a function of time (t) for different swimming velocities. (a) Large door size: $D = 67 \mu\text{m}$ ($\sim 7a$) the flux of particles increases when velocity is increased, the inset shows an equivalence between the flux q and the $\tau = \frac{a}{v}$ (Stokes time). (b) Small door size $D = 10 \mu\text{m}$ ($\sim a$) the flux is now decreasing when velocity is increased. The inset: Zoom showing the existence of plateaus, i.e., longer waiting times Δt .

left to right). The sampling window is located on the right-hand side (downstream) at $40 \mu\text{m}$ from the constriction with a width of $1.375 \mu\text{m}$ (1 px) and a height chosen as 1.5 times the diameter D [Fig. 1(a)]. Analyses are performed after a stable buildup is formed at the door with a volume fraction $\phi \approx 55\%$ to avoid any effect of density variation. Critical clogging (i.e., permanently clogged door) was never observed during our experiments. A stationary state characterized by a constant volume fraction at the constriction and cells exiting the constriction is observed along the whole duration of an experiment. However, experiments cannot be carried out on a duration exceeding 40 min as cells are observed to lose their sensitivity to light beyond this typical timescale.

Results. Effect of swimming velocity. This section focuses on the effect of swimming velocity on the evacuation process. With the velocity controlled and the data obtained as explained in the previous section, plotting the cumulative number of the escaping cells is straightforward. Our Letter focuses first on a wide door geometry with $D = 67 \mu\text{m} \sim 7a$. The cumulative number of cells escaping throughout the experiment plotted in Fig. 2(a) shows a linear trend where a more efficient evacuation occurs with higher swimming velocities. We define the flux q as the number of cells escaping per second. Graphically, it is the slope of linear fits. Figure 2(a) shows that the flux increases with increasing velocity, meaning the faster the cells swim the more they evacuate. Multiplying q by the Stokes time $\tau = \frac{a}{v}$ (the time that a cell takes to travel a distance equal to its own diameter) gives a value that is independent of velocity, hence, the equivalence between τ and q^{-1} . In the same method, when we analyze smaller door size $D = a = 10 \mu\text{m}$, results in Fig. 2(b) show a loss in linearity as V increases with the evacuation being more efficient for slower velocities and q increases with decreasing V .

In order to quantify jamming events, we study statistical distributions of time-lapses Δt [Fig. 3(b)] between two consecutive escaping CRs, known as the survival function,

$$P(t > \Delta t) = \int_{\Delta t}^{\infty} \rho(\Delta t') d\Delta t'.$$

where $\rho(\Delta t')$ is the distribution function of time lapses. F3 It has been argued [19] that a survival function following a power-law decay with an exponent equal to $1 - \alpha$ since $\rho(\Delta t) \sim \Delta t^{-\alpha}$

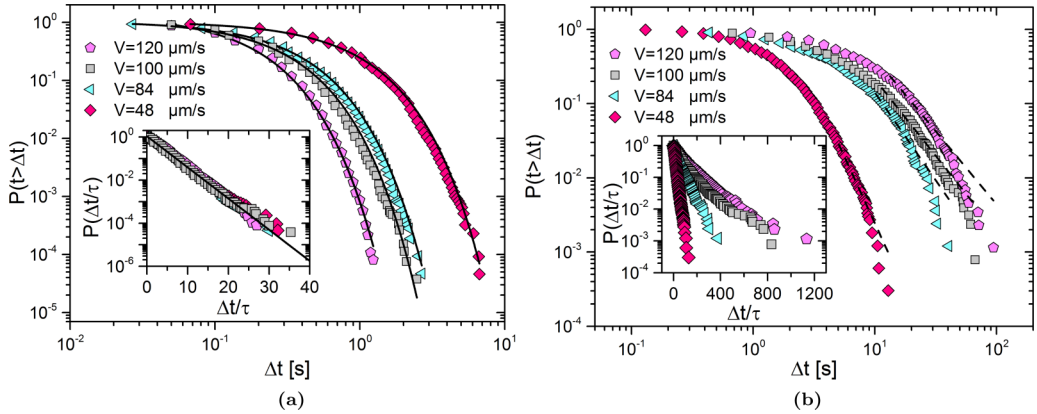


FIG. 3. Distribution of time lapses between two consecutive escaping CRs (survival function) for different swimming velocities. (a) $D = 67 \mu\text{m}$. Survival functions are well fitted by an exponential behavior (solid lines). The inset: log-lin representation shows a collapse when rescaling timescales by τ . (b) $D = 10 \mu\text{m}$ ($\sim a$). Survival functions show a power-law behavior (dashed lines). The inset: log-lin representation shows a deviation from exponential behavior and no collapse when timescales are rescaled by τ .

signifies that the system is susceptible to jam. On the other hand, an uninterrupted flow (i.e., flowing state) is represented by a survival function following an exponential decay (i.e., an average characteristic time lapse can then be defined).

Visually establishing a linear trend in a logarithmic-scaled histogram is not enough, therefore, the method described in Ref. [29], known as the Clauset-Shalizi-Newman method (CSN), and its corresponding open source code described in Ref. [30] are used to fit tails and extract values of α , the minimum time lapse above which the trend becomes power law (Δt_{\min}) and parameters determining the goodness of fit.

Figure 3(a) shows the survival function for different swimming velocities for $D = 67 \mu\text{m}$. For all velocities the dominating trend is that of an exponential decay $P(t > \Delta t) \sim \exp(-\frac{\Delta t}{T})$ describing a continuous, uninterrupted evacuation, T being the exponential time. Normalizing time lapses with τ in inset of Fig. 3(a), leads to a collapse of all velocities following an exponential decay (solid fit). Figure 3(b) shows the survival function for different swimming velocities for $D = 10 \mu\text{m}$. We note as the evacuation velocity increases, the probability to get longer time during which the flux is interrupted increases. In addition, when normalized by τ in the inset of Fig. 3(b), two distinct regimes can be seen. The first, for $\Delta t \leq \tau$, follows an exponential decay, describing a system that is more prone to a flowing state. The second, for $\Delta t > \tau$, the power-law trend prevails with a deviation from the exponential trend with no collapse when time is rescaled by τ and the system becomes more susceptible to jamming. Figure 4 shows that the coefficient α decreases with increasing V for $D < 50 \mu\text{m}$, this behavior is found in many systems and is compatible to what might be described as FiS.

On the other hand, the opposite behavior is observed for $D = 50 \mu\text{m}$. Figure 4 shows an increasing value of α with an increasing V , thereby the system is more prone to flow without jamming.

Effect of door width. In this section we are interested in the effect of door width on the evacuation process. The analysis is performed by fixing the swimming velocity whereas varying D . In the same procedure detailed in the previous section, we calculate the survival function and extract the coefficient α . Figure 4 shows that at constant V with increasing D , α increases as well. It means that the evacuation process is less susceptible to jamming, it is also well defined with the previous case of $D = 67 \mu\text{m}$. This observation gives a clue to the presence of a transition zone for $50 \mu\text{m} \leq D \leq 67 \mu\text{m}$. We would like to investigate the possibility of empirically calculating the value of a critical

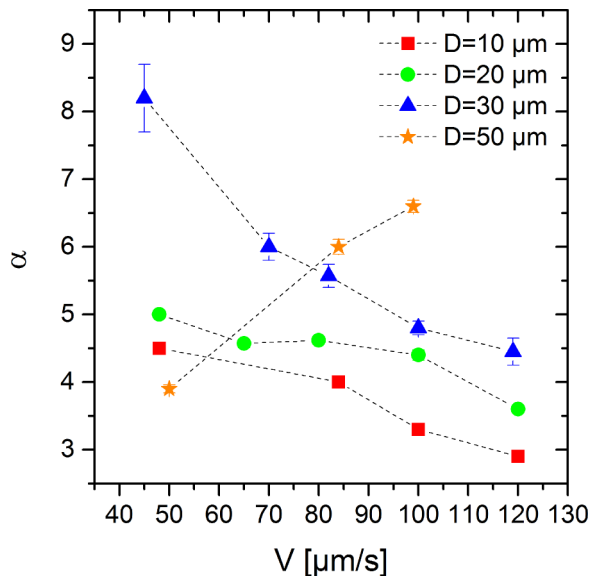


FIG. 4. Power-law exponent α of survival functions as function of swimming velocities and different door sizes. For small values of D ($<50 \mu\text{m}$), α decreases with V , whereas for $D = 50 \mu\text{m}$, α is found to increase with V . Error bars, when not visible, are smaller than symbols.

diameter D_c for which we obtain a transition from jamming to flowing state for a given velocity. A similar attempt was recently made for vibrated granular media in Ref. [31] where transition is dependent on the vibrating intensity and door size and in tilted hoppers [32] where the effect of the tilt angle is reported. But first, we need to tackle the problem of finding a Δt above which the system is considered jammed, noted as Δt_c . Such attempts have been performed in systems of sheep [33] and horizontal hoppers [34]. In our case we define $\Delta t_c = \Delta t_{\min}$ given by the CSN fitting method. For a door size $D = 10 \mu\text{m}$ and V varying from 48 to 120 $\mu\text{m/s}$, Δt_c varies from 3.15 to 12 s. We define the avalanche size s as the number of CRs that pass through the door between two jamming events, consequently, $\langle s \rangle$ is s averaged over the experiments for a waiting time Δt , we have a jamming if $\Delta t \geq \Delta t_c$. Having determined the way by which we obtain the avalanche size, we can now investigate the transition from flowing to jamming. Our results, the Supplemental Material [35], show that $\langle s \rangle$ grows with D , and the behavior can be described empirically by a power-law divergence, where $\langle s \rangle$ increases as D approaches its critical value D_c for which $\langle s \rangle$ diverges: $\langle s \rangle = \frac{C}{(D_c - D)^\beta}$ with D_c , C , and β being fitting parameters. Interestingly, work performed with three-dimensional silo [17] and tilted hoppers with different types of grains [32] shows a similar trend.

Another physical quantity that characterizes the state of the system is the jamming probability. In Ref. [36], the authors proposed a probabilistic model describing the behavior of avalanche size s of grains for gravity driven hoppers where jamming is due to arching. Even though we do not observe any arch formation in our experiments, we extend the reasoning to our system. Let us quantify avalanche size s with $\gamma(s)$ which is the probability of finding an avalanche of size s . By definition, an avalanche size consists of one jamming event and s nonjamming events. Therefore, we can write $\gamma(s) = p^s(1 - p)$. Here, p is the probability of a CR passing the door without cooperating with its neighbors to form a cluster and jam the door, $J = 1 - p$ is, therefore, the probability of a CR ability to jam the exit. We assume that p is constant for all CR given the uncorrelated nature of jamming structures. Thus, p is a fitting parameter extracted from experimental data fitted with the above expression of $\gamma(s)$, Supplemental Material [35]. p (and, subsequently, J) is dependent on both the door size D and the swimming velocity V .

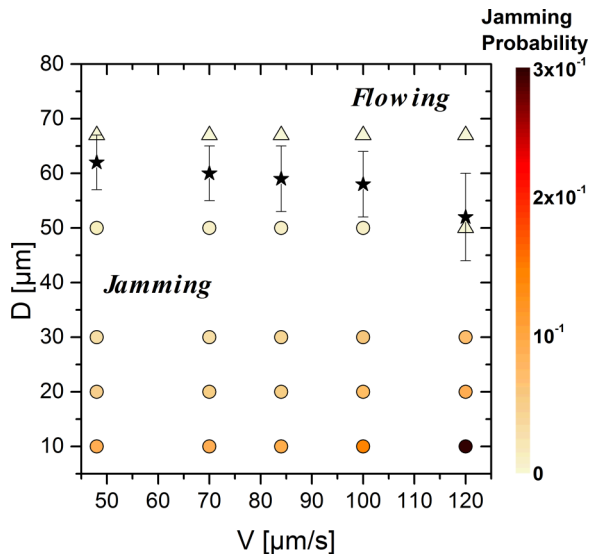


FIG. 5. Active jamming phase $D - V$. For $D < D_c$, a power-law behavior of the survival functions indicates jamming (\circ). For $D \geq D_c$, a flowing regime is found (Δ) and well described by exponential survival function. Values of D_c (\star) are given by $\langle s \rangle = \frac{C}{(D_c - D)^\beta}$ with error bars being the fitting confidence intervals. Jamming probability follows the color scale.

The phase diagram in Fig. 5 shows that the predicted values of D_c , extracted from the power-law divergence, are in agreement with our experimental results and fall well in the transition zone. In addition, it pin points the location of phase transition from a dominant power-law tail regime for $D < D_c$ where the system is prone to jam, to a domain dominated by an exponential decay for $D \geq D_c$ where the evacuation happens without observable interruption. The color indexing according to J gives an insight to the behavior of our system. Fixing D and increasing V shows an increase in jamming probability, whereas J decreases when fixing V and increasing D until reaching D_c above which $J = 0$.

Conclusion. To conclude, we have developed an experimental approach to study the active jamming of microswimmers at a constriction. We studied the effect of changing the swimming velocity and the opening size and looked at the results through two different points of view, the first being time-lapse distribution, the other being the avalanche size. We have found that the evacuation process for a given velocity is disturbed for a range of $D < D_c$, whereas for values of $D \geq D_c$ the system does not experience jamming. The approach used in studying granular systems describes well the effect of door size and swimming velocity on the jamming probability, suggesting underlying similarities in jamming issues between both granular and active suspensions. To gain further understanding of the mechanisms at hand in flowing to jamming transition in active suspensions, a thorough investigation of the cell-cell interactions, in particular, in the dense jammed suspensions would be fruitful.

Acknowledgments. We thank R. Mari and A. Nicolas for insightful discussions. We thank the CNRS 80Prime Program for financing this work. We thank the French-German University Program “Living Fluids” (Grant No. CFDA-Q1-14) (M.B., P.P., and S.R.)

[1] E. Matsumura, A. Nakagawa, Y. Tomabechei, S. Ikushiro, T. Sakaki, T. Katayama, K. Yamamoto, H. Kumagai, F. Sato, and H. Minami, Microbial production of novel sulphated alkaloids for drug discovery, *Sci. Rep.* **8**, 7980 (2018).

- [2] J. J. Milledge and S. Heaven, A review of the harvesting of micro-algae for biofuel production, *Rev. Environ. Sci. Bio/Technol.* **12**, 165 (2013).
- [3] A. Nakagawa, E. Matsumura, T. Koyanagi, T. Katayama, N. Kawano, K. Yoshimatsu, K. Yamamoto, H. Kumagai, F. Sato, and H. Minami, Total biosynthesis of opiates by stepwise fermentation using engineered *escherichia coli*, *Nat. Commun.* **7**, 10390 (2016).
- [4] W. C. DeLoache, Z. N. Russ, L. Narcross, A. M. Gonzales, V. J. Martin, and J. E. Dueber, An enzyme-coupled biosensor enables (s)-reticuline production in yeast from glucose, *Nat. Chem. Biol.* **11**, 465 (2015).
- [5] B. K. Hønsvall, D. Altin, and L. J. Robertson, Continuous harvesting of microalgae by new microfluidic technology for particle separation, *Bioresour. Technol.* **200**, 360 (2016).
- [6] A. Karimi, D. Karig, A. Kumar, and A. Ardekani, Interplay of physical mechanisms and biofilm processes: Review of microfluidic methods, *Lab Chip* **15**, 23 (2015).
- [7] C. R. Cabrera and P. Yager, Continuous concentration of bacteria in a microfluidic flow cell using electrokinetic techniques, *Electrophoresis* **22**, 355 (2001).
- [8] E. Dressaire and A. Sauret, Clogging of microfluidic systems, *Soft Matter* **13**, 37 (2017).
- [9] M. Hassanpourfard, R. Ghosh, T. Thundat, and A. Kumar, Dynamics of bacterial streamers induced clogging in microfluidic devices, *Lab Chip* **16**, 4091 (2016).
- [10] H. M. Wyss, D. L. Blair, J. F. Morris, H. A. Stone, and D. A. Weitz, Mechanism for clogging of microchannels, *Phys. Rev. E* **74**, 061402 (2006).
- [11] R. Mukhopadhyay, When microfluidic devices go bad, *Anal. Chem.* **77**, 429 A (2005).
- [12] I. Griffiths, A. Kumar, and P. Stewart, A combined network model for membrane fouling, *J. Colloid Interface Sci.* **432**, 10 (2014).
- [13] A. Marty, C. Roques, C. Causserand, and P. Bacchin, Formation of bacterial streamers during filtration in microfluidic systems, *Biofouling* **28**, 551 (2012).
- [14] A. Wolff, I. R. Perch-Nielsen, U. Larsen, P. Friis, G. Goranovic, C. R. Poulsen, J. P. Kutter, and P. Telleman, Integrating advanced functionality in a microfabricated high-throughput fluorescent-activated cell sorter, *Lab Chip* **3**, 22 (2003).
- [15] A. Lim and R. Bai, Membrane fouling and cleaning in microfiltration of activated sludge wastewater, *J. Membr. Sci.* **216**, 279 (2003).
- [16] D. Helbing, I. Farkas, and T. Vicsek, Simulating dynamical features of escape panic, *Nature (London)* **407**, 487 (2000).
- [17] I. Zuriguel, A. Garcimartín, D. Maza, L. A. Pagnaloni, and J. M. Pastor, Jamming during the discharge of granular matter from a silo, *Phys. Rev. E* **71**, 051303 (2005).
- [18] M. Souzy, I. Zuriguel, and A. Marin, Transition from clogging to continuous flow in constricted particle suspensions, *Phys. Rev. E* **101**, 060901(R) (2020).
- [19] I. Zuriguel, D. R. Parisi, R. C. Hidalgo, C. Lozano, A. Janda, P. A. Gago, J. P. Peralta, L. M. Ferrer, L. A. Pagnaloni, E. Clément *et al.*, Clogging transition of many-particle systems flowing through bottlenecks, *Sci. Rep.* **4**, 7324 (2014).
- [20] E. H. Harris, *The Chlamydomonas Sourcebook: Introduction to Chlamydomonas and Its Laboratory Use* (Academic Press, Oxford, 2009), Vol. 1.
- [21] M. Polin, I. Tuval, K. Drescher, J. P. Gollub, and R. E. Goldstein, *Chlamydomonas* swims with two “gears” in a eukaryotic version of run-and-tumble locomotion, *Science* **325**, 487 (2009).
- [22] M. Garcia, S. Berti, P. Peyla, and S. Rafaï, Random walk of a swimmer in a low-reynolds-number medium, *Phys. Rev. E* **83**, 035301(R) (2011).
- [23] X. Garcia, S. Rafaï, and P. Peyla, Light Control of the Flow of Phototactic Microswimmer Suspensions, *Phys. Rev. Lett.* **110**, 138106 (2013).
- [24] S. Rafaï, L. Jibuti, and P. Peyla, Effective Viscosity of Microswimmer Suspensions, *Phys. Rev. Lett.* **104**, 098102 (2010).
- [25] The effect of dextran addition on the cell-cell properties of adhesion and lubrication have, however, not yet been explored.
- [26] D. Qin, Y. Xia, and G. M. Whitesides, Soft lithography for micro-and nanoscale patterning, *Nat. Protoc.* **5**, 491 (2010).

- [27] D. B. Allan, T. Caswell, N. C. Keim, and C. M. van der Wel, trackpy Trackpy v0.4.1 (Zenodo, 2018), <https://doi.org/10.5281/zenodo.1226458>.
- [28] J. C. Crocker and D. G. Grier, Methods of digital video microscopy for colloidal studies, *J. Colloid Interface Sci.* **179**, 298 (1996).
- [29] A. Clauset, C. R. Shalizi, and M. E. J. Newman, Power-law distributions in empirical data, *SIAM Rev.* **51**, 661 (2009).
- [30] J. Alstott, E. Bullmore, and D. Plenz, powerlaw: A python package for analysis of heavy-tailed distributions, *PLoS ONE* **9**, e85777 (2014).
- [31] R. Caitano, B. V. Guerrero, R. E. R. González, I. Zuriguel, and A. Garcimartín, Characterization of the Clogging Transition in Vibrated Granular Media, *Phys. Rev. Lett.* **127**, 148002 (2021).
- [32] C. C. Thomas and D. J. Durian, Geometry dependence of the clogging transition in tilted hoppers, *Phys. Rev. E* **87**, 052201 (2013).
- [33] A. Garcimartín, J. M. Pastor, L. M. Ferrer, J. J. Ramos, C. Martín-Gómez, and I. Zuriguel, Flow and clogging of a sheep herd passing through a bottleneck, *Phys. Rev. E* **91**, 022808 (2015).
- [34] Q.-C. Yu, N. Zheng, and Q.-F. Shi, Clogging of granular materials in a horizontal hopper: Effect of outlet size, hopper angle, and driving velocity, *Phys. Rev. E* **103**, 052902 (2021).
- [35] See Supplemental Material at <http://link.aps.org/supplemental/10.1103/PhysRevFluids.7.L092301> show that $\langle s \rangle$ grows with D , and the behavior can be described empirically by a power-law divergence.
- [36] A. Janda, I. Zuriguel, A. Garcimartín, L. Pugnaroni, and D. Maza, Jamming and critical outlet size in the discharge of a two-dimensional silo, *Europhys. Lett.* **84**, 44002 (2008).